Final Project Report

Parallel Computing for Computational Mechanics

Johannes Grafen 380149
johannes.grafen@rwth-aachen.de

Abstract: A finite element method (FEM) based solver for the simulation of the unsteady heat equation on a two-dimensional disk is first optimized for serial performance and parallelized in a subsequent step. Three different meshes with different degrees of refinement were analysed. The performance analyses were conducted on Intel Platinum 8160 CPUs. The influence on the runtime of different compiler flags are tested and compared, where aggressive optimization with activation of the automatic vectorizer, using AVX512 instruction set extensions, showed the best performance gain. Parallelizations with OpenMP and MPI were assessed. For the OpenMP parallelization the two most time consuming loops were parallelized, achieving the highest performance with reduction clauses, with static scheduling and default chunk size. One-sided communication is used for the MPI-parallelization, with a round-robin partitioning. Different numbers of threads / cores are compared for each parallelization approach, regarding runtime, speed-up and efficiency. The obtained performance gain with the MPI parallelization was poor, as for a higher number of cores, no speed-up compared to the serial runtime could be observed. Improvements of the partitioning and the one-sided communication pattern are discussed.

Contents

List of Figures

List of Tables

1 Introduction

The optimization and the involved parallelization of code for the simulation of complex mechanical systems is a key-topic in modern computational mechanics. Constantly increasing computing power of high-performance clusters allow for the simulation of large and complex systems. This requires an efficient parallelization approach, where different parallelization paradigms can be of use.

In this report the optimization of a finite element method (FEM) code for the simulation of the unsteady heat equation on a two-dimensional disk is investigated. Therefore, first serial optimization is investigated, by evaluating the influence on performance gain of multiple compiler flags. In a next step the serial optimized code is parallelized using a shared memory approach with OpenMP and a distributed memory approach, using one-sided parallelization with MPI (Message Passing Interface). For the OpenMP (Open Multi-Processing) implementation, the performance gain with two different OpenMP directives (critical region and reduction) is analysed and compared. Different scheduling options with various chunk sizes are assessed and an optimum is determined. For the MPI implementation two different partitioning methods are discussed and possible improvements are presented.

Both parallelization approaches are assessed by evaluating the runtime, the speed-up and the efficiency for different number of threads / cores. The top speed-ups and efficiencies are determined for three different unstructured meshes, that are associated with three different refinement levels.

This report is structured as follows. In the second chapter *Theory and Methods* are presented, providing a short overview over the problem and presenting the finite element discretization. The *Implementation and Validation* of the presented problem is discussed in chapter 3, where excerpts of the code are shown and explained. The results for the coarse mesh are compared to an analytical solution for the problem, to validate the FEM solver. The results of the optimization of the runtime of the code is presented and discussed in chapter 4 *Results and Discussion*. Different optimization techniques and parallelization methods are assessed, determining the optimal number of threads for the OpenMP implementation and the optimal number of cores for the MPI implementation for each mesh. Finally, this report is closed with a *Conclusion* in which the key-findings are summarized in chapter 5 and possible further improvements are proposed.

2 Theory and Methods

2.1 Heat Equation and Problem Domain

From the final project assignment: The heat equation is solved on a disk Ω with the boundary Γ (Fig. 1) to obtain the radial temperature distribution. The Problem is given by the following heat equation, using Dirichlet boundary conditions at the disk outer boundary and an initial homogeneous Temperature T_0 on the whole disk:

$$\frac{\partial T}{\partial t} - \kappa \nabla^2 T = f \qquad \text{on } \Omega \ \forall t \in (0, t_f), \tag{1}$$

$$T(\mathbf{x}, t) = T_D \qquad \text{on } \Gamma \ \forall t \in (0, t_f), \tag{2}$$

$$T(\mathbf{x}, 0) = T_0 \qquad \text{on } \Omega. \tag{3}$$

where T is the temperature, κ the thermal diffusivity, and f the thermal heat source. The problem is solved for the time interval $t \in (0, t_f)$, with the final solution time t_f. The heat source is a function of the radius of the plate with:

$$f(r) = \begin{cases} \frac{Q}{\pi R_1^2} & \text{if } r < R_1, \\ 0 & \text{if } r \geq R_1 \end{cases} . \tag{4}$$

where $Q = P \cdot d_z$ is the volumetric heat source and $d_z = 0.1m$ the out-of-plane thickness. For validation purposes an analytical solution for $t \to \infty$ is given by:

$$T(r) = \begin{cases} T_0 - \frac{Q}{2\pi\kappa}\left(\frac{1}{2}\left(\frac{r^2}{R_1^2} - 1\right)\right) + ln\left(\frac{R_1}{R_2}\right) & \text{if } r < R_1, \\ T_0 - \frac{Q}{2\pi\kappa} ln\left(\frac{r}{R_2}\right) & \text{if } r \geq R_1 \end{cases} . \tag{5}$$

The parameters for the specific heated disk problem are provided in Tab. 1.

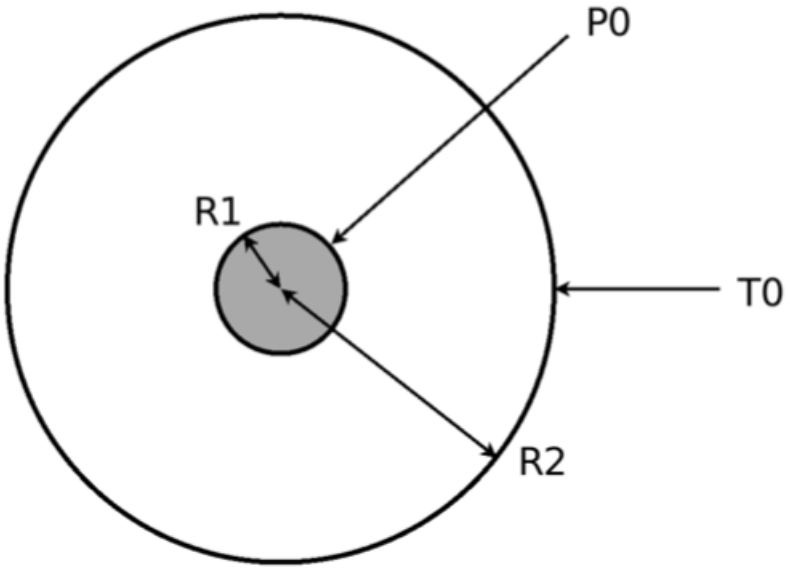

Figure 1: Problem domain

2.2 Weak Form

To obtain a discrete formulation in space and time for a finite element discretization for the unsteady heat equation, a weak or variational form of Eq. (1) has to be defined. Two sets of function spaces

Parameter	Variable	Value	Unit
Inner circle radius	R_1	0.01	$[m]$
Outer circle radius	R_2	0.1	$[m]$
Heat source on the area	Q	100	$[W]$
Dirichlet BC temperature	$T_0(x, y)$	500	$[K]$
Initial temperature	$T_s(x, y, 0)$	0	$[K]$
Thermal diffusivity	κ	1.0	$[m^2/s]$

Table 1: Problem parameters for the heated disk problem

have to be defined in the context of the standard Galerkin formulation [1]:

$$\mathcal{V} = \{w \in \mathcal{H}^1(\Omega) | w = 0 \text{ on } \Gamma_D\} \tag{6}$$

$$\mathcal{S} = \{T \in \mathcal{H}^1(\Omega) | T = T_D \text{ on } \Gamma_D\} \tag{7}$$

where the space $\mathcal{V}$ is composed of test functions that are square integrable and have square integrable first derivatives over the computational domain Ω. They vanish on the Dirichlet boundary Γ_D. The set of functions $\mathcal{S}$ are the trial solutions. This collection of functions has similar properties to the test functions, except that those functions have to satisfy the Dirichlet boundary condition on the domain boundary Γ_D. $\mathcal{S}$ and $\mathcal{V}$ are both continuous function spaces. For the finite element method these function spaces are approximated by finite dimensional subsets $\mathcal{S}^h$ and $\mathcal{V}^h$.

The weak formulation of Eq. (1) is given as:

$$\int_\Omega w \frac{\partial T}{\partial t} d\Omega - \kappa \int_\Omega w \nabla^2 T d\Omega = \int_\Omega w f d\Omega \quad \forall w. \tag{8}$$

By applying the Green-Gauss divergence theorem on the left-hand-side (LHS) of Eq. (8), the order of the spatial derivatives can be reduced. Together with a zero homogeneous Neumann boundary condition ($n \cdot \nabla T = 0$ on Γ_h), we obtain the following equation:

$$\int_\Omega w \frac{\partial T}{\partial t} d\Omega + \kappa \int_\Omega \nabla w \cdot \nabla T d\Omega = \int_\Omega w f d\Omega \tag{9}$$

2.3 Finite Element Method

The discretized variational formulation of the continuous PDE in weak form (Eq. (9)) that is used for the FEM, is formulated as: find $T^h \in \mathcal{S}^h$, such that $\forall w^h \in \mathcal{V}^h$

$$\sum_{B \in \eta \backslash \eta_D} \left[(N_A, N_B) \frac{\partial T_b}{\partial t} + a(N_A, N_B) T_B \right] = (N_A, f) - \sum_{B \in \eta_D} a(N_A, N_B) T_D(\mathbf{x}_B), \forall A \in \eta \backslash \eta_D. \tag{10}$$

with

$$T^h(\mathbf{x}) = \sum_{B \in \eta} N_B(\mathbf{x}) T_B, \tag{11}$$

where N_A are the shape functions used for the interpolation of the continuous weighting function $w(x, y)$, N_B are the shape functions for the interpolation of $T(x, y)$, $a(N_A, N_B)$ represents the discretized thermal diffusive part of the equation (second term on left-hand-side in Eq. (9)) and (N_A, f) denotes the discretized version of the right-hand-side. η represents the set of all nodes and η_D is a subset of η containing all nodes on the boundary, where the Dirichlet boundary condition is applied.

This variational formulation leads to a matrix form of equations:

$$[M]\left\{\dot{T}\right\} + [K]\left\{T\right\} = \left\{F\right\} \tag{12}$$

where M refers to the mass matrix, K to the stiffness matrix and F to the source vector. After applying a first order explicit time integration scheme and isolating the LHS by inverting the mass matrix M the explicit equation to obtain the temperature at the nodes for a time step n can be written as:

$$\{T\}^{n+1} = ([M]^n)^{-1}([M]^n\{T\}^n + \Delta t(\{F\}^n - [K]^n\{T\}^n) \tag{13}$$

In a first step the mass matrices are computed on element level and then assembled globally. To solve the integrals efficiently in combination with the unstructured grid, an isoparametric approach is chosen. Therefore, the integrals are evaluated on a triangular reference element. To map the results back to the physical domain, the transformation theorem is applied:

$$\int_{\Omega^e} \Phi(\mathbf{x}) d\mathbf{x} = \int_{\Omega^{ref}} \Phi(\xi, \eta))|\mathbf{J}(\xi, \eta)| d\xi d\eta \tag{14}$$

Φ denotes an arbitrary function in $\mathcal{S}$, $\mathbf{J}$ the Jacobian for the transformation between global coordinates (x, y) and the reference coordinates (ξ, η), Ω^e the physical element domain and Ω^{ref} the reference domain of the element. The integrals are solved numerically by using Gaussian quadrature:

$$\int_0^1 \int_0^{1-\eta} \Phi(\xi, \eta) d\xi d\eta \approx \sum_{i=1}^{n_{quad}} w_i \Phi(\xi_i, \eta_i) \tag{15}$$

with weights w_i and ξ_i, η_i, the quadrature points at which $\Phi(\xi, \eta)$ is determined. The individual entries of the matrices M, K and F are then calculated as follows:

$$M^e_{i,j} = \sum_{m=1}^{n_{quad}} w(m) S_i(\xi_m \eta_m) S_j(\xi_m, \eta_m) |\mathbf{J}_m|, \tag{16}$$

$$K^e_{i,j} = \kappa \sum_{m=1}^{n_{quad}} w(m)(\partial_x S_i(\xi_m, \eta_m))\partial_x S_j(\xi_m, \eta_m) + \partial_y S_i(\xi_m, \eta_m)\partial_y S_j(\xi_m, \eta_m)|\mathbf{J}_m|, \tag{17}$$

$$F^e_i = \sum_{m=1}^{n_{quad}} w(m) f S_i(\xi_m, \eta_m) |\mathbf{J}_m|. \tag{18}$$

For an efficient inversion of the mass matrix, which is necessary to obtain the spacial temperature distribution for the next time step (Eq. (13)), mass lumping is used. This technique is an approximation of the original system, transforming the mass matrix into a diagonal matrix, which can be stored as a vector.

2.4 Meshes

For the FEM Solver, three different unstructured meshes are used with different refinement levels (coarse, medium and fine). The number of nodes and elements of the three different unstructured triangular meshes (coarse, medium and fine) are presented in Tab. 2.

mesh	number nodes (nn)	number elements (ne)
coarse	2041	3952
medium	21650	21332
fine	85290	84656

Table 2: Number of nodes and elements for the three different meshes

3 Implementation and Validation

3.1 Convergence Criterion

The unsteady solution of the heat equation converges to a steady-state for $t \to \infty$. In order to break out of the time loop a convergence criterion has to be defined, which states the change of the temperature between two subsequent time steps:

$$\epsilon_{RMS} = \sqrt{\frac{1}{nn}\sum_{i=1}^{nn}\left(T_i^{n+1} - T_i^n\right)^2} \leq 10^{-7} \tag{19}$$

with the root-mean-square error ϵ_{RMS} and the number of nodes $nn \in \eta \backslash \eta_D$. If ϵ_{RMS} is lower than a predefined error (10^{-7}), the simulation is declared as converged and is finished.

3.2 Serial Code

The calculation of the element matrices is performed as presented in Eq. (16) to Eq. (18). The corresponding code is illustrated in Code excerpt 1. The values of the shape functions and their derivatives, as well as the determinate of the Jacobian is precomputed for each element node, before entering the iteration loop. The matrices M, K and F are computed on element level. After performing the mass lumping procedure the element level matrices must be hard-copied to the corresponding triangular element. Then the Dirichlet boundary condition Eq. (2) is applied at the domain boundary nodes. The global mass for each node is accumulated.

Listing 1: Calculation of Element Matrices

```
1  // First, fill M, K, F matrices with zero for the current element
2  (...)
3
4  // Now, calculate the M, K, F matrices
5  for(int p=0; p<nGQP; p++)
6  {
7      (...)
8      for(int i=0; i<nen; i++)
9      {
10         for(int j=0; j<nen; j++)
11         {
12             // Consistent mass matrix
13             M[i][j] = M[i][j] +
14             mesh->getME(p)->getS(i) * mesh->getME(p)->getS(j) *
15             mesh->getElem(e)->getDetJ(p) * mesh->getME(p)->getWeight();
16             // Stiffness matrix
17             K[i][j] = K[i][j] +
18             D * mesh->getElem(e)->getDetJ(p) * mesh->getME(p)->getWeight() *
19             (mesh->getElem(e)->getDSdX(p,i) * mesh->getElem(e)->getDSdX(p,j) +
20             mesh->getElem(e)->getDSdY(p,i) * mesh->getElem(e)->getDSdY(p,j));
21         }
22         // Forcing matrix
23         F[i] = F[i] + factor_F * mesh->getME(p)->getS(i);
24
25     }
26 }
27
28 //Calculation of total mass and the total diagonal mass and perform mass lumping
29 (...)
30
31 //Total mass at each node is accumulated on local node structure:
```

```
32 for(int i=0; i<nen; i++)
33 {
34     node = mesh->getElem(e)->getConn(i);
35     mesh->getNode(node)->addMass(M[i][i]);
36 }
37
38 // At this point we have the necessary K, M, F matrices as a member of femSolver
39 // object.
40 // They must be hard copied to the corresponding triElement variables.
41 for(int i=0; i<nen; i++)
42 {
43     node = mesh->getElem(e)->getConn(i);
44     mesh->getElem(e)->setF(i, F[i]);
45     mesh->getElem(e)->setM(i, M[i][i]);
46     for(int j=0; j<nen; j++)
47     {
48         mesh->getElem(e)->setK(i,j,K[i][j]);
49     }
50 }
```

After the previous computations the explicit solver is entered. The outer loop is an iteration loop in which the convergence criterion Eq. (19) is checked at the end (Code excerpt 2). If convergence is reached, the code breaks out of the loop. After clearing all entries of the RHS storage *MTnew*, the second inner loop iterates over all elements, evaluating the RHS at element level (line 9 to 22 in Code excerpt 2). This is followed by the computation of the new temperature, using the inverted mass matrix, which inverse corresponds to it's reciprocal as the mass lumping algorithm was previously applied to diagonalize the mass matrix. Subsequently, the global RMS error can be computed and the convergence criterion Eq. (19) is checked.

Listing 2: Explicit Solver

```
1     for (int iter=0; iter<nIter; iter++)
2     {
3         // clear RHS MTnew
4         (...)
5         // Evaluate right hand side at element level
6         for(int e=0; e<ne; e++)
7         {
8             (...)
9             for(int i=0; i<nen; i++)
10            {
11                TL[i] = T[elem->getConn(i)];
12            }
13
14            MTnewL[0] = M[0]*TL[0] + dT*(F[0]-(K[0]*TL[0]+K[1]*TL[1]+K[2]*TL[2]));
15            MTnewL[1] = M[1]*TL[1] + dT*(F[1]-(K[3]*TL[0]+K[4]*TL[1]+K[5]*TL[2]));
16            MTnewL[2] = M[2]*TL[2] + dT*(F[2]-(K[6]*TL[0]+K[7]*TL[1]+K[8]*TL[2]));
17
18            // RHS is accumulated at local nodes
19            MTnew[elem->getConn(0)] += MTnewL[0];
20            MTnew[elem->getConn(1)] += MTnewL[1];
21            MTnew[elem->getConn(2)] += MTnewL[2];
22        }
23
24        // Evaluate the new temperature on each node on partition level
25        partialL2error = 0.0;
26        globalL2error = 0.0;
27        for(int i=0; i<nn; i++)
```

```
28          {
29              pNode = mesh->getNode(i);
30              if(pNode->getBCtype() != 1)
31              {
32                  massTmp = massG[i];
33                  MT = MTnew[i];
34                  Tnew = MT/massTmp;
35                  partialL2error += pow(T[i]-Tnew,2);
36                  T[i] = Tnew;
37                  MTnew[i] = 0;
38              }
39          }
40          globalL2error = sqrt(partialL2error/this->nnSolved);
41          globalL2error = globalL2error / initialL2error;
```

3.3 Parallelization with OpenMP

The two most time consuming loops, which are the computation of the RHS and the computation of the global RMS error, are to be parallelized on loop-level with a shared memory approach. This means multiple threads share the work of the operations inside a loop, and have access to the same memory address space.

Therefore OpenMP directives are used. Two different approaches are implemented, denoted with "A)" and "B)" which are assessed in Sec. 4.2.1. The corresponding directives are presented in Code excerpt 3.

For approach "A)", *MTnew* is declared as *firstprivate* upon entry in the parallel region. This ensures, that the entries *MTnew* are initialized at the entry of the parallel section, which means *MTnew* is copied from the parent thread to the child threads. For approach "B)", no initialization of *MTnew* is performed on the child threads, as it is a *shared* array among all threads. Both approaches declare the element object *elem*, the mass matrix M, the stiffness matrix K, the source vector F, the local temperature TL, the node loop index i and the local RHS *MTnewL* as *private*. This means all these objects are *private* (local) to the thread and undefined upon entry to the region. For approach A), *critical* region are used for the accumulation of the RHS at the local nodes and the computation of the partial L2 errors.

A *critical* region is executed by only one thread at a time. This is important to prevent data races. A data race means that multiple threads try to access and manipulate the same variable / memory address at the same time. This might lead to unpredictable behavior, which can result in incorrect computations.

For approach B), *reduction* operations are used. The *reduction* operation for the computation of the RHS at element level for each element node, allows each thread to first compute local sums of the each *MTnew* entry in parallel and then performs a serial summation of all local sums to obtain the value of an *MTnew* entry. But this serial summation is only computed once, compared to the *critical* region. The same procedure applies also for the computation of the *partialL2error*.

In this context different scheduling options, with different chunk sizes can be compared (Sec. 4.2.2). Explaining the different scheduling options briefly, "static" scheduling accounts for a static chunk size, meaning a chunk is consisting of a constant number of iterations. These chunks are then distributed in a round-robin fashion among the threads. "Dynamic" scheduling however allows the chunk size to be allocated dynamically, based on the load of a thread. "Guided" scheduling works similar to dynamic scheduling, but with a chunk size that is constantly decreasing, based on the unassigned iterations left. The scheduling option "auto" leaves this decision to the compiler.

Listing 3: Parallelization of two most time consuming loops with implementation A and B

```
1     for (int iter=0; iter<nIter; iter++)
2     {
3         // clear RHS MTnew
4         A) #pragma omp parallel for
5         B) #pragma omp parallel for
6         for(i=0; i<nn; i++){
7             MTnew[i] = 0;
8         }
9         A) #pragma omp parallel firstprivate(MTnew)
10        B) #pragma omp parallel
11        {
12            // Evaluate right hand side at element level
13            A) #pragma omp for private(elem, M, F, K, TL, i, MTnewL)
14            B) #pragma omp for private(elem, M, F, K, TL, i, MTnewL)
15            B) reduction(+: MTnew[0:nn]) schedule(dynamic,512)
16            for(int e=0; e<ne; e++)
17            {
18                elem = mesh->getElem(e);
19                M = elem->getMptr();
20                F = elem->getFptr();
21                K = elem->getKptr();
22                for(i=0; i<nen; i++)
23                {
24                    TL[i] = T[elem->getConn(i)];
25                }
26
27                MTnewL[0] = M[0]*TL[0] + dT*(F[0]-(K[0]*TL[0]+...));
28                MTnewL[1] = M[1]*TL[1] + dT*(F[1]-(K[3]*TL[0]+...));
29                MTnewL[2] = M[2]*TL[2] + dT*(F[2]-(K[6]*TL[0]+...));
30
31
32                // RHS is accumulated at local nodes
33                A) #pragma omp critical
34                MTnew[elem->getConn(0)] += MTnewL[0];
35                A) #pragma omp critical
36                MTnew[elem->getConn(1)] += MTnewL[1];
37                A) #pragma omp critical
38                MTnew[elem->getConn(2)] += MTnewL[2];
39            }
40            // Evaluate the new temperature on each node on partition level
41            partialL2error = 0.0;
42            globalL2error = 0.0;
43            A) #pragma omp for private(pNode, massTmp, MT, Tnew)
44            B) #pragma omp for private(pNode, massTmp, MT, Tnew)
45            B) reduction(+:partialL2error) schedule(dynamic,512)
46            for(int i=0; i<nn; i++)
47            {
48                pNode = mesh->getNode(i);
49                if(pNode->getBCtype() != 1)
50                {
51                    massTmp = massG[i];
52                    MT = MTnew[i];
53                    Tnew = MT/massTmp;
54                    A) #pragma omp critical
55                    partialL2error += pow(T[i]-Tnew,2);
56                    T[i] = Tnew;
57                }
```

```
58              }
59          }
60
61          globalL2error = sqrt(partialL2error/nn);
```

3.4 Parallelization with MPI

The other parallelization approach that is investigated for the presented FEM solver is a distributed memory approach. Therefore, the message passing interface communication (MPI) is used, with one-sided communication. This communication pattern assumes a machine with direct memory access hardware, like for most shared memory computers and a few distributed memory machines. The participating processors (PEs) inside a MPI communicator need to know the memory layout of each other. This has the benefit, that more complex procedures like send and receive operations, as in two-sided communication, can be circumvented. But this also means that this method is more error prone as the processors have access to each others memory.

For an adequate distribution of the data and the computation, first the partitioning has to be determined. It should be aimed for an even distribution, as the load is balanced among all PEs that way. The number of elements on the current PE, the possible maximum number of elements, the number of nodes on the current PE and the maximum number of nodes are computed as presented in Code excerpt 4.

Listing 4: Determination of number elements on current rank and number nodes in current

```
1   // Determine nec, mec
2   nec = (ne-1)/npes + 1;
3   mec = nec;
4   if ((mype+1)*mec > ne)
5   nec = ne - mype*mec;
6   if (nec < 0)
7   nec = 0;
8
9   // Determine nnc, mnc
10  nnc = (nn-1)/npes + 1;
11  mnc = nnc;
12  if ((mype+1)*mnc > nn)
13  nnc = nn - mype*mnc;
14  if (nnc < 0)
15  nnc = 0;
```

The coordinate data of all nodes and the connectivity of the nodes to form the elements is read from different grid input files. The code in Code excerpt 5 shows the data input exemplary. Each processors reads a nearly equal amount of data with a certain offset from the input file in parallel and stores it to it's local memory.

Listing 5: Read file for every rank with specific offset

```
1   (...)
2   offset = mype*nsd*mnc*sizeof(double);
3   MPI_Type_contiguous(nnc*nsd, MPI_DOUBLE, &mxyzftype);
4   MPI_Type_commit(&mxyzftype);
5   MPI_File_open(MPI_COMM_WORLD, writable, MPI_MODE_RDONLY,
6   MPI_INFO_NULL, &fileptr);
7   MPI_File_set_view(fileptr, offset, MPI_DOUBLE, mxyzftype,
8   "native", MPI_INFO_NULL);
9   readStream = new char [nsd*nnc*sizeof(double)];
10  MPI_File_read(fileptr,readStream, nsd*nnc, MPI_DOUBLE, &status);
11  swapBytes(readStream, nsd*nnc, sizeof(double));
```

```
12      for(int i=0; i<nnc; i++)
13      {
14          node[i].setX(*((double*)readStream + nsd*i));
15          node[i].setY(*((double*)readStream + nsd*i+1));
16          xyz[i*nsd+xsd] = *((double*)readStream + nsd*i);
17          xyz[i*nsd+ysd] = *((double*)readStream + nsd*i+1);
18      }
19      if (mype==0) cout << "> File read complete: " << dummy << endl;
20
21      MPI_File_close(&fileptr);
22      MPI_Barrier(MPI_COMM_WORLD);
```

As every PE contains a certain number of node objects and element objects in its memory, the nodes are in general not the nodes that are associated with the elements. Therefore, global data of the associated element nodes has to be distributed to each PE. A certain procedure is applied in order to create a mapping from local nodes to the global nodes, which will not be explained in detail for the sake of brevity.

The explicit solver is parallelized using MPI as illustrated in Code excerpt 6. The basic operations are the same as for the serial solver. Every processor evaluates the RHS *MTnewL* for it's local elements nodes. After the computation of the local RHS *MTnewL* for each local element nodes, an MPI accumulation is executed, which adds up all the computed values of *MTnewL* for a specific global node to obtain *MTnewL*, as multiple elements can share a global node, which is therefore part of multiple PE. This is always the case for the nodes at partition boundaries.

After the new temperatures are computed for each time step on a global level, the temperature has to be distributed back to the local node level in *localizeTemperature* in line 31 in Code excerpt 6. The global error can then be determined with a *MPI_Allreduce*, adding up all partial errors for each partition and distributing the result back to all PEs inside the MPI communicator.

Listing 6: Explicit solver for MPI parallelization

```
1       MPI_Win winMTnew;
2       MPI_Win winTG;
3
4       MPI_Win_create(MTnewG, nnc*sizeof(double), sizeof(double), MPI_INFO_NULL,
5       MPI_COMM_WORLD, &winMTnew);
6       MPI_Win_create(TG, nnc*sizeof(double), sizeof(double), MPI_INFO_NULL,
7       MPI_COMM_WORLD, &winTG);
8       MPI_Win_fence(0, winMTnew);
9       MPI_Win_fence(0, winTG);
10
11      localizeTemperature(winTG);
12
13      for (int iter=0; iter<nIter; iter++)
14      {
15
16          // Similar to serial Code, RHS is evaluated at element level
17          // and accumulated at local nodes
18          (...)
19
20          // local node level MTnew is transferred to partition node level
21          // (MTnewL to MTnewG)
22          accumulateMTnew(winMTnew);
23
24          // Evaluate the new temperature on each node on partition level
25          for(int i=0; i<nnc; i++)
26          {
27              pNode = mesh->getNode(i);
28              (...)
```

```
29          }
30
31          // Transfer new temperatures from partition to local node level
32          // (from TG to TL)
33          localizeTemperature(winTG);
34
35          MPI_Allreduce(&partialL2error, &globalL2error, 1, MPI_DOUBLE, MPI_SUM,
36          MPI_COMM_WORLD);
37
38          globalL2error = sqrt(globalL2error/(double)this->nnSolved);
39
40          // Output of iterations and globalL2error on parent processor
41
42      MPI_Win_free(&winMTnew);
43      MPI_Win_free(&winTG);
44
45      (...)
```

For the partitioning, different ways are possible. A partitioning in round-robin fashion is opposed to a symmetric partitioning is discussed in Sec. 4.3.2

3.5 R1 a) Validation

For the validation of the FEM solver, the solution of the coarse mesh is compared to the analytical solution Eq. (5) in Fig. 2. The numeric solution is in good agreement with the analytical solution. Slight deviations are observed at the disk's center where the temperature distribution has it's global maximum. This accounts for large changes in the temperature gradient at the center of the disk, which require a finer mesh in order to be better resolved.

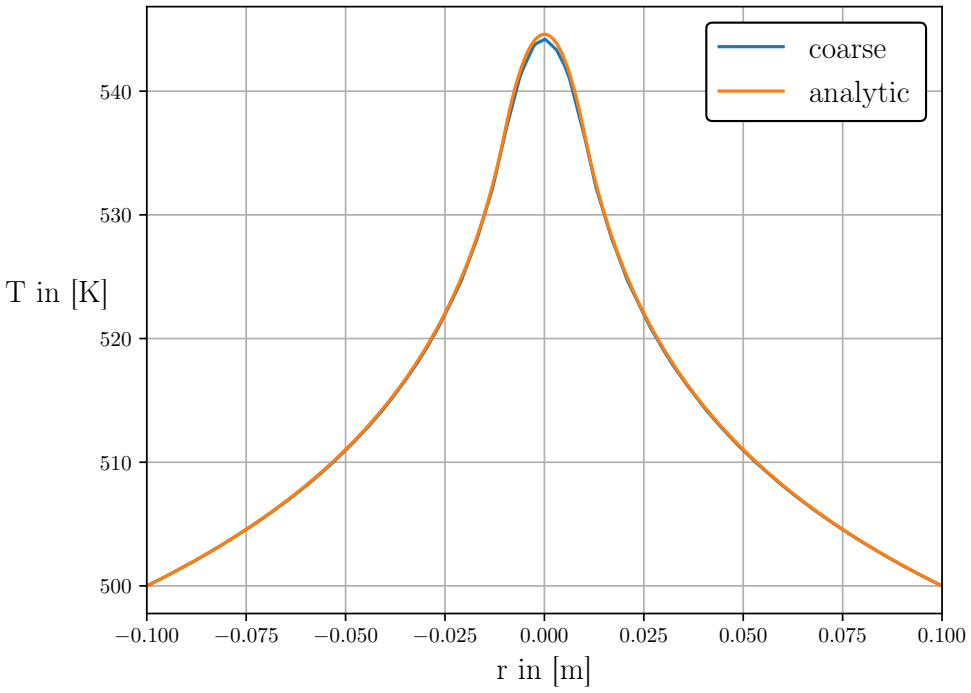

Figure 2: Comparison of the steady-state temperature distribution of the analytical solution (Eq. (5)) and the numerical solution on the coarse mesh

4 Results and Discussion

4.1 Serial Solver

To run the FEM solver as efficient and fast as possible in parallel, it is important that the serial performance is optimized. Therefore, the effects on the runtime of multiple compiler flags are compared in this section.

4.1.1 R1 a)

In order to decrease the serial runtime of the implemented solver, different compiler flags were tested and assessed by comparing their influence on the solver runtime. The code is compiled with the Intel C++ Compiler (v19.1). The compiled code is tested on a Intel Platinum 8160 which is based on Intel's Skylake architecture using the "medium" unstructured mesh with 21650 nodes resulting in 21332 triangular elements Tab. 2.

The investigated compiler flags are contained in Tab. 3. In the following subsection the individual compiler flags are briefly presented and explained:

-O0

The number behind the capital "O" refers to the optimization level and performs general optimizations by bundling several individual compiler flags. Using the base Level (0), the compiler will disable all optimizations. This is useful for debugging (Sec. 4.1.1).

-O1

Optimization Level 1 includes the optimization for speed, but disables all optimizations that increase code size and affect the code's speed. It includes the analysis of data-flow, code motion, strength reduction and further performance enhancing options.

-O2

The second optimization level includes vectorization, which allows for concurrent execution of the separate steps that are necessary to perform different basic mathematical operations on array-like data structures. Such as an element-wise addition of an array. A scalar or "Von Neumann" processor would simply perform all four necessary steps for each index step by step. Where as a vector processor allows for concurrent operations. This prevents that instruction units are idle, while waiting on a task to be finished.

The option also enables the inlining of intrinsics and intra-file inlining of functions. Which means the replacement of the function call with the instructions inside of a certain function itself. This can cause significant performance gain, especially if functions are called multiple times inside the body of a loop.

-O3

Performs O2 optimizations with higher thresholds and enables more aggressive loop transformations such as Fusion, Block-Unroll-and-Jam, and collapsing IF-statements. It can be used with the option "-ax" to force the compiler to do a more aggressive data dependency analysis and optimize for a certain CPU architecture. Where "x" refers to the CPU's instruction set extensions.

-Ofast

On Linux systems this sets "-O3 -no-prec-div -fp-model fast=2". This causes the compiler to enhance the code with alle possible optimizations of "-O3" and reduce the precision of floating-point divides.

-ax *arch*

Activation of the automatic vectorizer of the compiler, enabling code generation for processors that employ the vector operations contained in AVX and other instruction set extensions . The simulations were conducted on a two-socket node with two Intel Platinum 8160 with each 24 cores, based on the Skylake architecture. The shortest runtime was achieved with the flag "-axSKYLAKE-AVX512". Where AVX512 is the abbreviation for *Advanced Vector Extensions* with 512-bit instructions and is an extension of the SIMD instruction set for vector operations.

-fp-model fast

This flag controls the precision of floating-point operations. Using Level 2, enables a more aggressive optimization of floating-point calculations. This might decrease accuracy.

-ipo

Enables the inter-procedural optimization between files. Functions from different files may be inlined.

-unroll

Performs loop unrolling, which helps to exploit multiple instruction units, by increasing the stride length of the loop variable and performing the same operation on multiple array elements in one stride.
[2, 3, 4, 5]

The runtimes that were measured for the different compiler flags are shown in Tab. 3. For each flag, three measurements on a single core with a single thread were taken and the average time was determined. The shortest runtime is achieved by using the compiler flag combination "-O3 -axSKYLAKE-AVX512" resulting in an average runtime of 54.77 seconds which is 4.37 times faster that the not optimized code (-O0). For further investigations, assessing the parallel optimization with OpenMP and MPI, the "-O3 -axSKYLAKE-AVX512" flag combination was used.

4.1.2 R1 b)

A higher level of optimization can cause a decrease in the accuracy of the floating-point operations. For the validation of a certain code or high fidelity simulations, like the implemented FEM Solver, one is advised to minimize the numerical error, by using the highest level of accuracy. So the optimizations should not inflict with the desired results. Also for debugging purposes, optimization is not helpful as the compiler changes the code structure, when using more aggressive optimizations. To name a few effects: functions are inlined, loops are unrolled or fused together. This makes is very hard to search for bugs, when using debugging software.

compiler flag	time 1	time 2	time 3	average time
-O0 (no optimization)	233.71	241.5	243.02	239.41
-O1	62.41	63.71	62.76	62.96
-O2	56.96	55.39	57.11	56.49
-O3	55.49	55.23	57.8	56.17
-O3 -axSSE4.2, SSSE3, SSE2 -fp-model fast=2	56.17	56.21	56.46	56.18
-O3 -fp-model fast=2	57.69	56.19	57.89	57.26
-O3 -axSKYLAKE-AVX512	53.99	54.06	56.25	**54.77**
-O3 -ipo	54.57	57.26	60.38	57.40
-unroll	55.17	57.01	55.94	56.04
-Ofast	55.43	56.17	56.27	55.96

Table 3: Timings of the various compiler flags for serial optimization, the shortest achieved runtime is printed in bold font

4.2 Parallel OpenMP Solver

In this section the performance gain by parallelization with OpenMP of the two most time consuming loops is investigated (Code excerpt 3). For each time measurement in this section three timings were taken and averaged.

4.2.1 R2 a)

First, two different OpenMP parallelization approaches are compared an discussed. The approaches are denoted with "A)" and "B)" in the Code excerpt 3. Approach A) uses *critical* regions, which are executed by each thread serially for the computation of the RHS at element-level and the partial-L2-errors. Where as approach B) is performing a *reduction* operation for the determination of *MTnew* and the *partialL2error*, using a "dynamic" scheduling with a chunk size of 512 iterations for both loops.

To compare both approaches, the runtimes for the simulation of the temperature distribution on the coarse mesh is determined for 1, 2 and 4 threads for each parallelization approach. Three runtimes were measured per thread count and averaged. As presented in Fig. 3, the runtimes of the approach A) (Fig. 3a) for different number of threads is in general significantly higher than the runtimes of approach B) (Fig. 3b), with a top runtime of 142.59 seconds for a run with 4 threads for approach A and a runtime of 1.01 seconds for approach B. The scaling behavior of approach B was found to be as theoretically expected, as the runtime decreases with an increasing number of threads. Due to the very short runtimes the run with 2 threads was measured to be slower than a run with only a single thread. This requires further investigations as possible fluctuations in the runtime, for instance due to memory access, are in the order of the runtime itself. Approach A shows the opposite dependency of thread number and runtime. The runtime increases with an increasing number of threads.

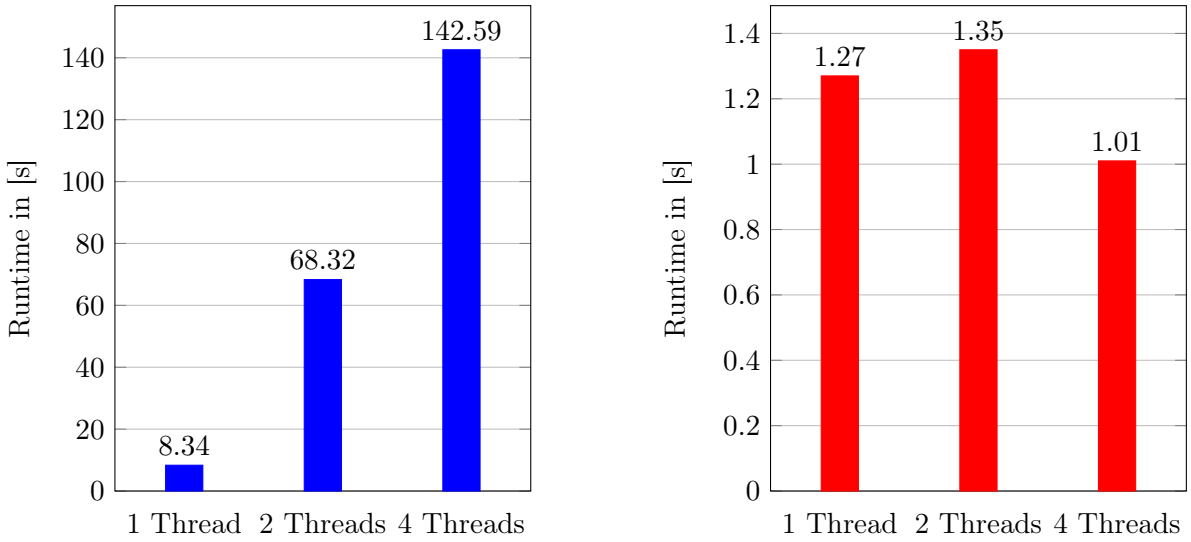

(a) OpenMP approach A **(b)** OpenMP approach B

Figure 3: Timings for solver with different OpenMP optimizations on the coarse mesh

As the *critical* regions of approach A) are to be executed by only one thread at a time, the runtime will increase with an increasing number of threads, as observed in Fig. 3a. A large overhead is created due to the management of locks, to ensure that only one thread at a time is running through a *critical* region. This overhead increases with a higher number of threads. While one thread is executing a *critical* region the other threads have to wait for this specific thread to finish this section. Only if this thread has completely finished the computations inside a *critical* region the next thread is allowed to execute this region for it's assigned loop indices. To prevent the overhead of multiple locks and to allow threads to work in parallel the *reduction* keyword for OpenMP is used in approach B), which is explained in Sec. 3.3.

4.2.2 R2 b)

To further optimize the parallelization with OpenMP, different scheduling options and chunk sizes are investigated for approach B) (Code excerpt 3). Therefore simulations on the fine mesh with a constant number of 4 threads were conducted. Some unexplained behavior was observed, when using scheduling options, other than static for the second loop in which the partial-L2-errors are computed, where the L2 error gets initialized again with 0, which leads to an untimely convergence of the simulation. Therefore, different scheduling options and chunk sizes were first only applied for the first loop (line 15 Code excerpt 3) for the computation of the RHS on element level. For the second loop (line 45 Code excerpt 3) a static scheduling with default chunk size was used. The results are presented in Fig. 4. In general the static scheduling for the *reduction*-clause of the first loop performs best with a shortest runtime of 184.06 seconds for a chunk size of 256 iterations. In general larger runtimes are observed for the dynamic and guided scheduling options. For dynamic scheduling a larger chunk size of 512 iterations leads to shorter runtimes, where as for static and guided scheduling the medium chunk size of 256 iterations performs best. The runtime of the auto scheduling is at 220.97 seconds, which is marked in gray in Fig. 4.

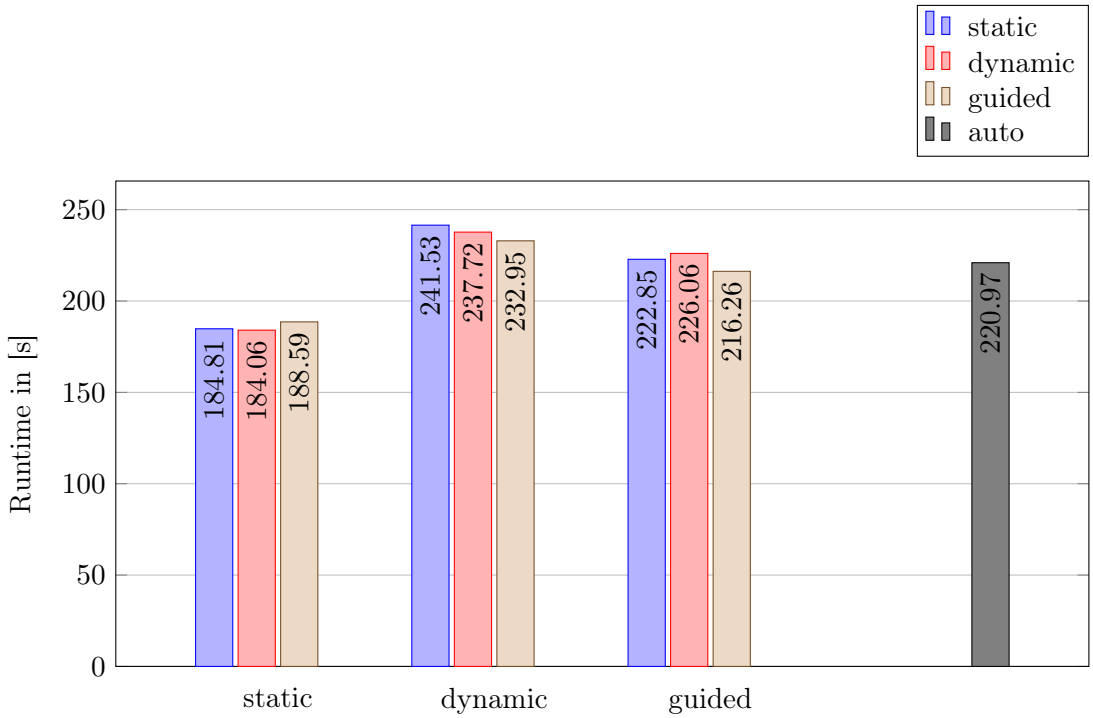

Figure 4: Comparison of different scheduling options (static, dynamic, guided, auto) for different chunk sizes(128, 256, 512) in the first parallelized loop for 4 threads on the finest mesh

In addition to the introductory investigations regarding the different scheduling options, static scheduling was inspected further. Therefore, the *reduction* operations for the parallelization of the first and second loop are both equipped with static scheduling and similar chunk size. The effects of the different chunk sizes are compared in Fig. 5. The runtime is decreasing with an increasing chunk size. The shortest runtime is observed for the default option in scheduling, with 177.21 seconds on average, which divides the number of loop iterations by the number of threads. This results in a chunk size of 21164 iterations for the first loop and in a chunk size of 21322.5 iterations on average for the second loop for the fine mesh with 85290 nodes and 84656 elements (Tab. 2). Thus, the static scheduling with the default chunk size is used for the calculation of speed-up and efficiency for the different meshes in the following section.

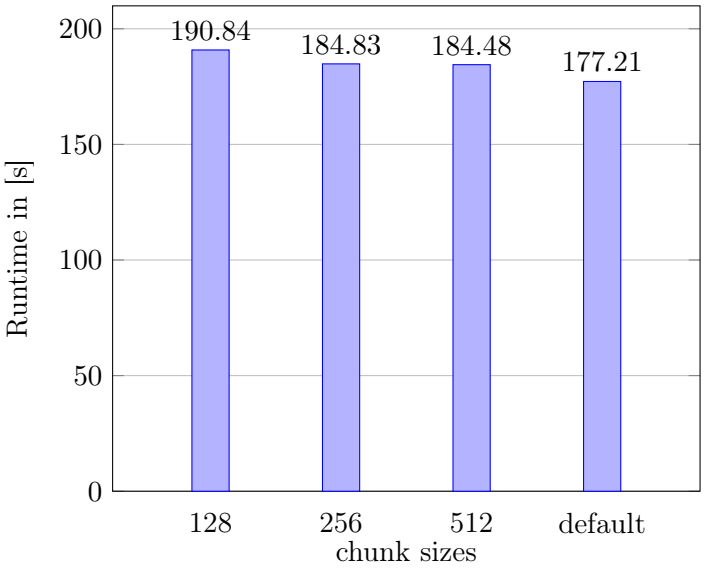

Figure 5: Runtimes for parallelization of loop in line 15 and loop in line 45 in Code excerpt 3 with static scheduling and different chunk sizes

4.2.3 R2 c)

To evaluate the performance gain of approach B) with static scheduling and default chunk size, the runtime, the speed-up (Eq. (20)) and the efficiency (Eq. (21)) are computed for 1, 2, 4, 6, 8, 10 and 12 threads and plotted in Fig. 6 and Fig. 7. The speed-up is defined as

$$S_p = \frac{T_1}{T_p} \ , \tag{20}$$

where T_1 denotes the serial runtime of the respective code and T_p the time of parallelized code with p number of threads (processors when considering MPI). The Efficiency is defined as the quotient of speed-up and number of threads / processors

$$E_p = \frac{S_p}{p} \ . \tag{21}$$

Ideal efficiency would correspond to $E_p = 1$, which means a direct proportional dependency of speed-up and number of processors. This means x number of processors would result in an x times faster code in comparison to the serial code. Ideal efficiency and speed-up can not be achieved in a real situation. First, there are always parts of the code that just can be executed serially or have to be executed by each thread. Second, there will always be some overhead or idle time, if threads are waiting for other threads to complete their tasks at the end of parallel regions. If time is the most important feature, speed-up has to be considered. If the core-hours are to be minimized and used most efficiently, the efficiency should be the measure of choice.

In Fig. 6 the different runtimes for the different simulations on three different meshes (coarse, medium, fine) are visualized. For the coarse mesh the shortest runtime was found for 8 threads with 1.13 seconds (Fig. 6a). In comparison to the medium (Fig. 6b) and fine grids (Fig. 6c), which show good scaling behavior, with a monotonously decreasing runtime for an increasing number of threads. The maximum runtime for the coarse mesh was found for 2 threads with 1.5 seconds, which is also visible in the speed-up and efficiency plots, showing larger values for two threads as expected. For a higher number of threads the runtime is expected to decrease, resulting in a speed-up smaller or ideally equal to the number of threads p and an efficiency smaller or ideally equal to 1 (100%). Therefore, the measurement for two threads was not considered in the determination of optimal speed-up and efficiency for the coarse mesh. This behavior can contributed to the short runtime of the simulations

on the coarse mesh itself, as they are in the order of possible fluctuations. Also the number of loop iterations is for the coarse grid not high enough, that parallelization would pay off. For the medium mesh the shortest runtime is 22.42 seconds with 10 threads and 107.75 seconds for the fine mesh, obtained with 12 threads.

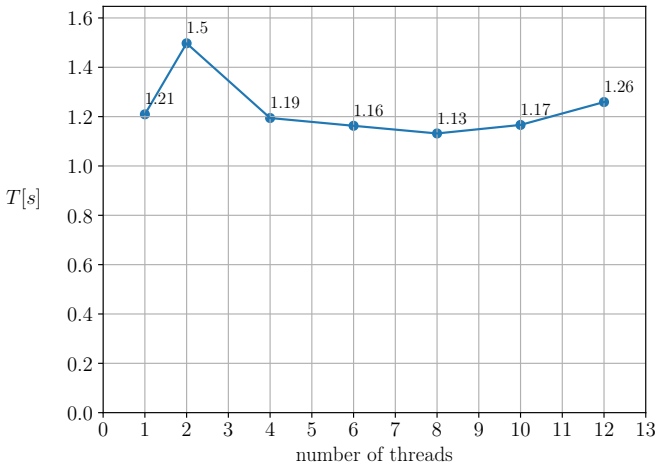

(a) coarse mesh

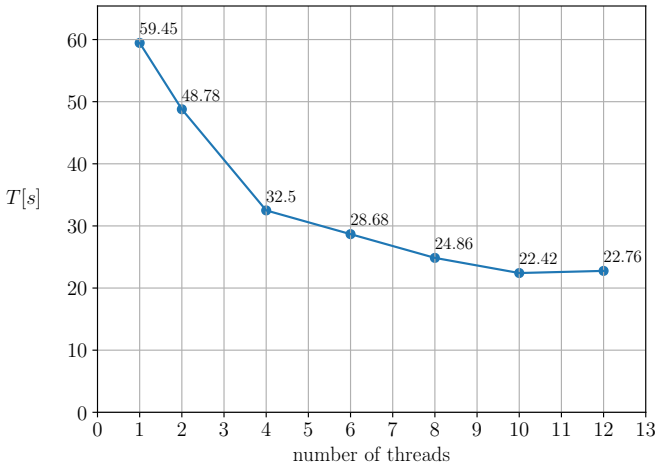

(b) medium mesh

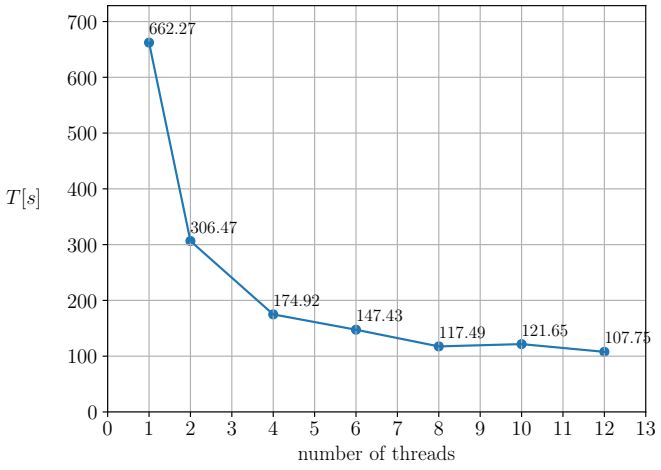

(c) fine mesh

Figure 6: Runtime for coarse, medium and fine mesh for different number of threads

Overall the highest speed-up is observed for 12 threads on the fine mesh with a 6.15 times faster execution than the serial runtime. This corresponds to an efficiency of 0.51. The fine mesh shows the highest speed-up and efficiencies for the different number of threads. This is due to the amount of computations. The coarse mesh has not enough elements and nodes to achieve great performance gain through parallelization as the overhead gets fast to large for a higher number of threads. This results in 8 threads being fastest for the coarse mesh, where as 10 threads for the medium mesh and 12 threads for the fine mesh provide the fastest execution time (Fig. 7).

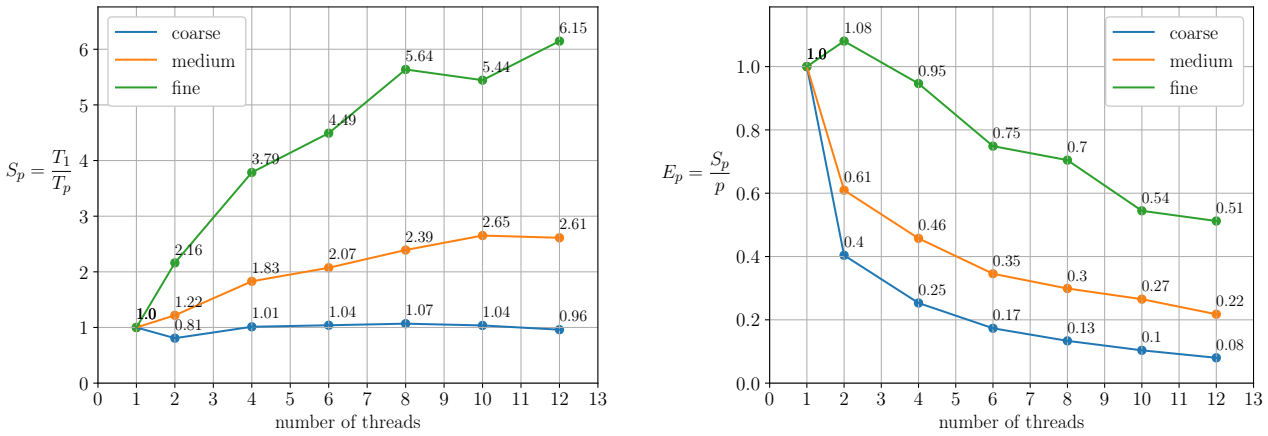

(a) Speed-up **(b)** Efficiency

Figure 7: Speed-up and efficiencies for coarse, medium and fine mesh for different numbers of threads

4.2.4 R2 d)

This short subsection is dedicated to the default values of the chunk sizes for different scheduling methods. The default scheduling for OpenMP usage on an Intel compiler is static. The default chunk size of static is determined by the quotient of the number of loop iterations and the number of threads. For dynamic scheduling the default chunk size is 1. Lastly, the default chunk size for guided scheduling is proportional to the number of unassigned iterations divided by the number of the threads. This means the chunk size dynamically decreases for guided scheduling. The scheduling option auto delegates the decision of the scheduling type to the compiler or runtime of the system [6].

4.3 Parallel MPI Solver

In this section the MPI parallelization of the FEM Solver is examined regarding it's parallel performance.

4.3.1 R3 a)

Fig. 8 presents the different runtimes for three different meshes that have different levels of refinement. The FEM code was run for 1, 2, 4, 6, 8, 12 and 16 cores, using the compiler flags for best serial performance (Sec. 4.1).

For the coarse mesh the shortest average runtime is at 1.52 seconds with 2 cores (Fig. 8a), for the medium mesh at 64.69 seconds also with 2 cores (Fig. 8b) and for the fine mesh at 342.57 seconds, which is achieved with 4 cores (Fig. 8c).

In Fig. 9, speed-up and efficiency are illustrated for the different meshes. As already observed in the runtime plots, the best speed-up for the coarse and medium mesh is obtained with 2 cores with a speed-up of 1.26 and 1.22, respectively. For the fine mesh the parallelized code runs fastest with 4 cores, resulting in a speed-up of 2.32. The efficiency graphs show an expected development, as the efficiency monotonically decreases with an increasing number of threads. For the MPI parallelization with 2 cores on the fine mesh a noticeable high efficiency of 100% was measured, being at optimum efficiency, marked in orange in (Fig. 9f). This means that 2 cores do not introduce nearly any communication overhead and a perfect scaling behavior can be achieved. For the highest number of cores all meshes show a very poor efficiency between only 1-8%. A main influence is potentially the used partitioning approach, which is discussed in (Sec. 4.3.2). Again the same principle applies for distributed memory parallelization. If time is the priority, then according to the speed-up plots, 2 cores should be chosen for the coarse and medium mesh and 4 cores for the fine mesh. If, on the other hand the core-hours are limited and the simulations are supposed to be as efficient as possible, a serial code execution would be most efficient for coarse and the medium mesh. For the fine mesh two cores would be optimal regarding efficiency as they showed excellent scaling behavior.

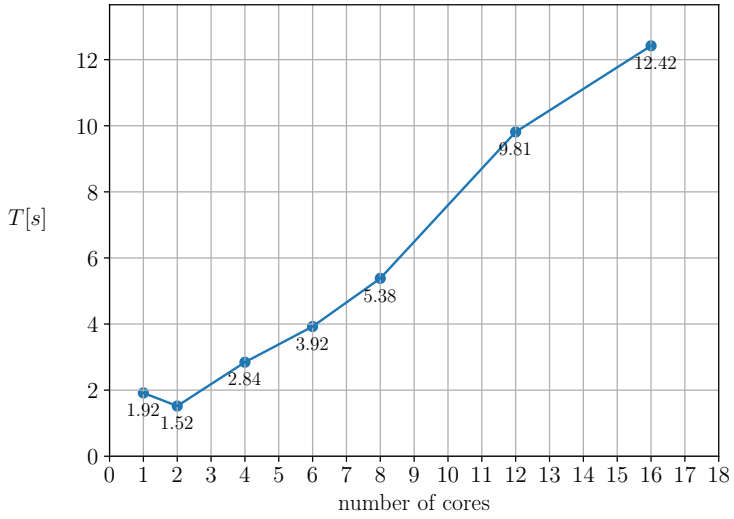

(a) coarse mesh

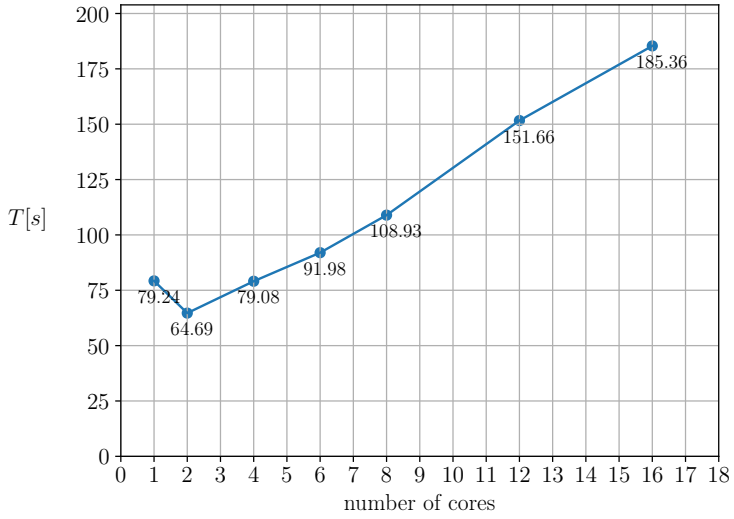

(b) medium mesh

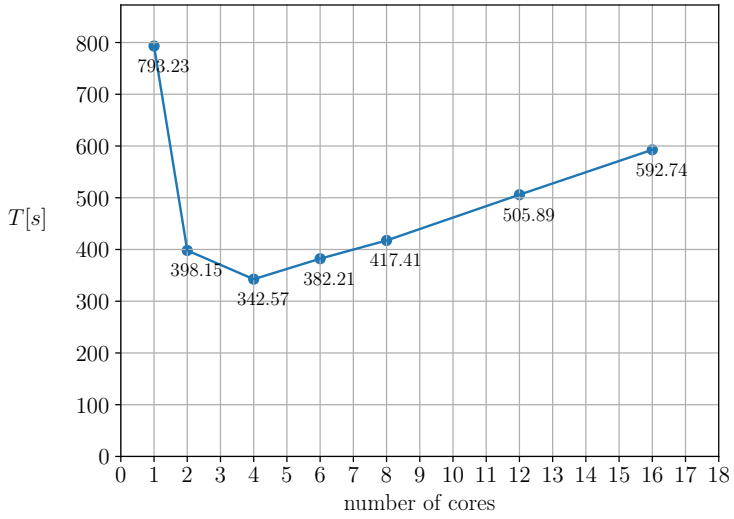

(c) fine mesh

Figure 8: Runtime for coarse, medium and fine mesh for different number of cores

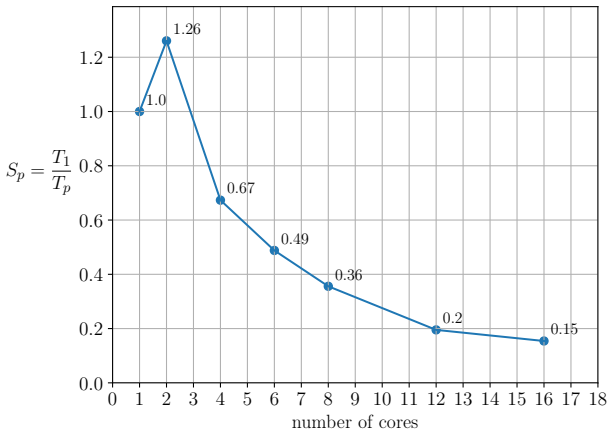

(a) Speed-up coarse mesh

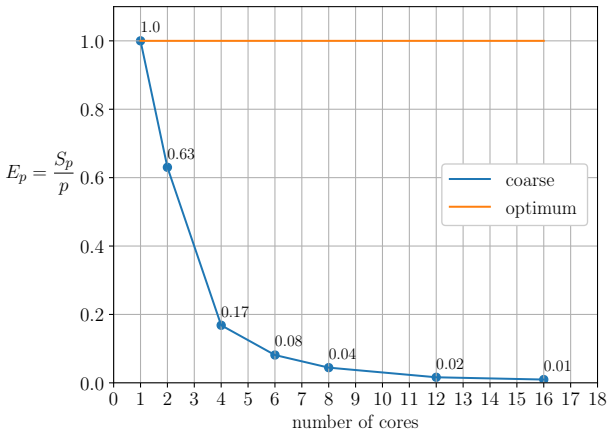

(b) Efficiency coarse mesh

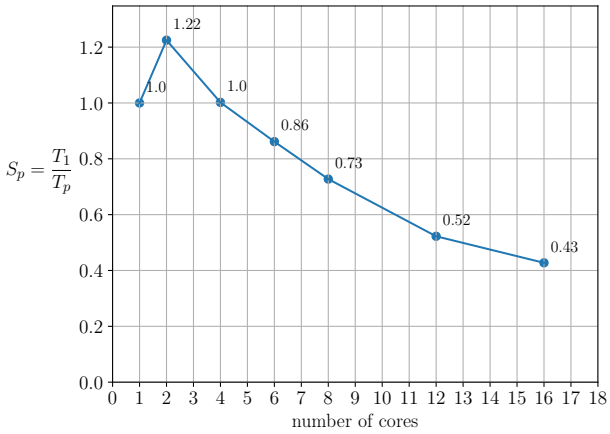

(c) Speed-up medium mesh

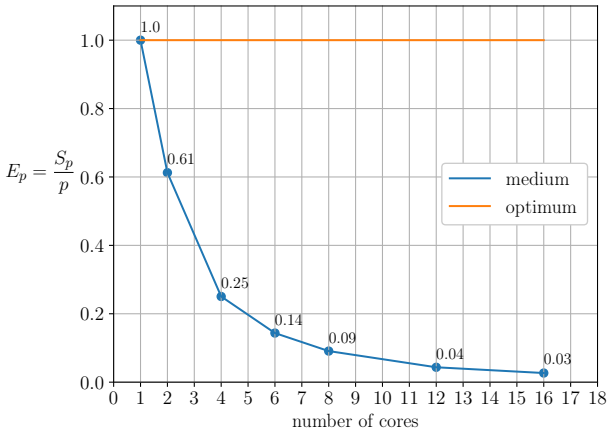

(d) Efficiency medium mesh

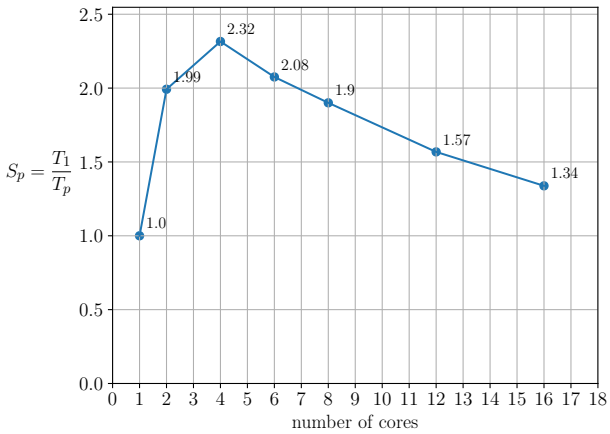

(e) Speed-up fine mesh

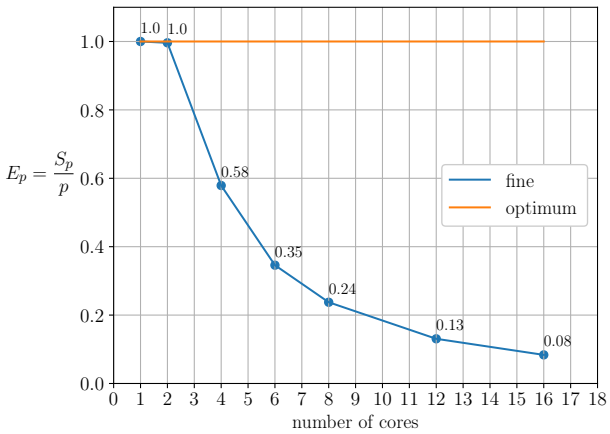

(f) Efficiency fine mesh

Figure 9: Speed-up and efficiency for coarse, medium and fine mesh for different number of cores

4.3.2 R3 b)

The partitioning of the elements and nodes of the mesh among the individual cores is performed in a round-robin fashion, depending on how the mesh data structure is stored in the mesh input file. Each processor reads with a certain offset a specific amount of elements and nodes from this input file, that is distributed as evenly as possible among the different cores. This results in a more irregular distribution as it can be seen from Fig. 10. This partitioning is far from optimal as it is in general recommended to use a partitioning with minimum boundary surfaces between different partitions. This will reduce the necessary communications between neighboring partitions. For a circular domain, like the investigated heat diffusion problem on a flat circular plate, a distribution of p identical circle sectors is advisable, where p represents the number of processors used. This partitioning would minimize the boundary surfaces between the partitions.

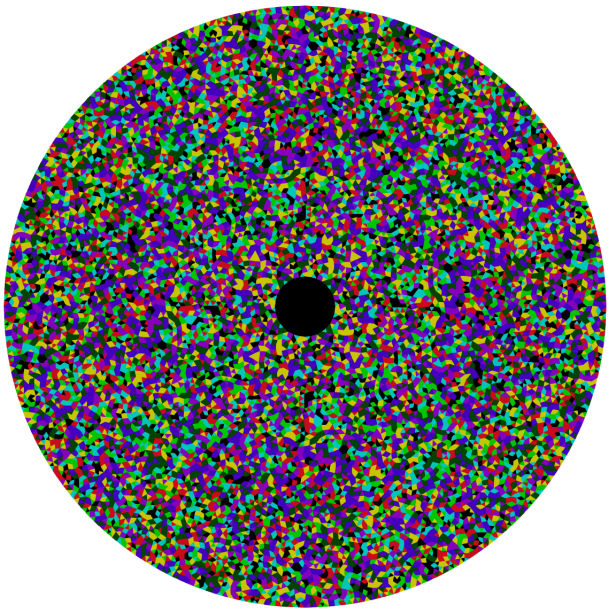

Figure 10: Partitioning of medium mesh using 8 cores, the different colors indicate the affiliation to different partitions

4.3.3 R3 c)

The overall performance of the code can be improved. Some speed-up is achieved, with the shortest runtime for two cores for the coarse and medium mesh and for four cores for the fine mesh. However the efficiency is poor, especially for a higher number of cores (Fig. 9). The current bottleneck is the communication overhead. A lot of loops (line numbers) run over all processors, which results in an increasing loop size for an increasing number of processors. Inside these loops a lot of MPI calls occur, which will result in high communication overhead. Therefore, some kind of static data structure, which stores information for all nodes could help. Also a window-halo approach would be beneficial, which allows certain processors to store some data of directly neighboring elements and nodes, that are required for an efficient communication. This method could efficiently be implemented in combination with a two-sided communication pattern, where only direct neighbor partitions have to exchange data. This would especially pay-off for a high number of processors and therefore partitions, as the two-sided approach does not require loops over all partitions, just for the direct neighbors.

Another way to improve the performance of the code is to couple shared memory parallelization on a loop level with OpenMP with the distributed memory parallelization with MPI on global mesh level. Meaning the loops, especially for computing the RHS on element level and for the computation

of the L2 error can be parallelized with the proposed approach B) (Code excerpt 3) on each processor. So each processor executes, or at least creates, multiple threads. This approach is then called hybrid parallelization.

4.3.4 R3 d)

This section answers some general question regarding MPI commands and communication methods:

1) Why do we use *MPI_Accumulate* in the code instead of *MPI_Put*?

With the *MPI_Accumulate* function a reduction among all the processors of a certain variable or array elements can be performed. Like a summation or finding the maximum value throughout all processors. *MPI_Put* simply overwrites a value.

2) What are the advantages of using one-sided MPI communication over two-sided MPI communication?

On one hand, one-sided communication has no risk of deadlocks as the individual processors do not have to wait for send and receives of other processors in a communicator. Also the communication patterns are in general easier to implement for one-sided communication. On the other hand, the processors simply can read and write to another processor's memory that is made accessible by the MPI window. This however, is error prone and requires a thought-through communication. Two-sided communication is more time-consuming or cumbersome to implement. But, through the send and receive approach, data encapsulation is ensured and the programmer is always aware of which data is exchanged between individual processors. But blocking methods that are required for two-sided communication can lead to an increase in waiting time.

3)What advantage does MPI offer over OpenMP, what is a main obstacle of MPI?

The difference in the MPI and the OpenMP parallelization approaches lies in the memory architecture. MPI is designed for a distributed memory approach, which does not make any limitations to the number of processors to be used. In contrast, OpenMP follows the shared memory approach, so this make the physical memory of a CPU the limitation for the number of threads. But the parallelization with OpenMP is less complex as compiler directives can be easily added to existing code, when considering loop parallelization. MPI introduces a lot of additional overhead, when writing parallel code, due to specific MPI commands and the partitioning.

4.4 Overall Best Performance

Overall the highest speed-ups are achieved with the OpenMP parallelization for the fine and medium mesh. With a speed-up of 6.15 for the fine mesh with 12 threads, a speed-up of 2.65 with 10 threads for the medium mesh. For the coarse mesh, the MPI parallelization showed the highest speed-up for 2 cores with 1.26, with also the highest efficiency of 0.63 for the coarse mesh. This means the shared memory approach of OpenMP is more efficient for a higher number of threads in combination with more loop iterations, as the fine and medium meshes contain more elements. Not as much data has to be exchanged, as it is already available. The MPI implementation has more communication overhead opposed to OpenMP, but seems to be the better choice for the coarse mesh. As the investigations for the scheduling option and the chunk sizes were conducted on the fine mesh, a different scheduling approach with a different chunk size might be more optimal for the coarse mesh. Therefore, further investigations would be necessary. As for now the OpenMP approach was only optimized on the fine mesh and was proven to help for a higher performance gain, than with the MPI implementation on the fine mesh.

5 Conclusion

In this report, a FEM solver was optimized and parallelized by first applying serial optimizations with different compiler flags and then comparing two different parallelization paradigms. The performance on three different meshes was analysed and evaluated and an optimum of the thread count and core count for the different parallelization approaches was determined.

For the serial optimization, the compiler flag "-O3 -axSKYLAKE-AVX512" was found to enhance the performance of the FEM solver most, providing the shortest serial runtime. This compiler flag uses the most aggressive level of optimization for the used Intel C++ Compiler, combined with an optimized instruction set for the specific hardware, which is an Intel Platinum 8160, based on Intel's Skylake architecture, using 512-bit SIMD instructions.

The optimal compiler flag was then used in combination with a parallelization with OpenMP. The two most time consuming loops were parallelized, with the reduction clause showing better performance opposed to the critical section. Combined with a static scheduling and default chunk size, the shortest runtime and therefore the highest speed-up was found for 8 threads on the coarse mesh, 10 threads on the medium mesh and 12 threads on the fine mesh. The highest efficiencies were achieved with 2 threads on each mesh.

Using a one-sided communication approach with a round-robin partitioning for the parallelization with MPI, the runtime plots as well as speed-up and efficiency plots were generated. The highest speed-up was achieved with 2 cores on the coarse and medium meshes and with 4 cores on the fine mesh. With a monotonically decreasing efficiency for an increasing number of processors. The overall performance gain is poor, as the partitioning is not optimal, because the boundary surfaces between the individual partitions is not minimized. There is room for improvement using a more symmetric partitioning, like circular sections for the disk-shaped domain. The one-sided communication pattern requires looping over all processors inside a communicator, this procedure is increasing the runtime as the number of cores inside the MPI communicator is increased. For a higher number of cores a two-sided communication approach might be more efficient. Overall, the OpenMP parallelization showed the highest performance gain for the fine mesh, with a speed-up of 6.15 and an efficiency of 0.51 for 12 threads. Also for the medium mesh, the best improvement in performance was achieved with OpenMP, where as the MPI approach performed better for the coarse mesh. For further performance gain a hybrid parallelization with a combination of MPI and OpenMP would be desirable for future studies.

References

[1] J. Donéa and Antonio Huerta. *Finite Element Methods for Flow Problems*. Wiley, Chichester ; Hoboken, NJ, 2003.

[2] Dieter an Mey, Christian Terboven, Paul Kapinos, Dirk Schmidl, Sandra Wienke, and Tim Cramer. The RWTH HPC-Cluster User's Guide Version 8.4.0.

[3] Marek Behr. Lecture: Parallel Computing for Computational Mechanics.

[4] Quick Reference Guide to Optimization with Intel® C++ and Fortran Compilers v19.

[5] Intel® C++ Compiler Classic Developer Guide and Reference, April 2022.

[6] Jaka Špeh. OpenMP: For & Scheduling, June 2016.